

Quantum current magnification in a multi-channel mesoscopic ring

Swarnali Bandopadhyay,^{1,*} P. Singha Deo,^{1,†} and A. M. Jayannavar^{2,‡}

¹*S. N. Bose National Centre for Basic Sciences, JD Block,
Sector III, Salt Lake City, Kolkata 700098, India.*

²*Institute of Physics, Sachivalaya Marg, Bhubaneswar 751005, India*

(Dated: March 13, 2021)

We have studied the current magnification effect in a multi-channel open mesoscopic ring. We show that the current magnification effect is robust even in the presence of several propagating modes inspite of mode mixing and cancellation effects. The magnitude of circulating currents in the multi-channel regime can be much larger than that in a single channel case. Impurities can enhance or degrade the current magnification effect depending sensitively on the system parameters. Circulating currents are mostly associated with Fano resonances in the total transport current. We further show that system-lead coupling qualitatively changes the current magnification effect.

PACS numbers: 73.23.-b, 72.10.-d, 72.10.Bg

Keywords: current magnification, multi-channel, transport current

I. INTRODUCTION

In the light of recent developments in fabrication techniques it has become possible to make metallic or semiconductor structures having dimensions of a few atomic spacings. The typical size of the systems can be made smaller than the phase coherence length of the electron. Such mesoscopic systems are important for their possible device applications as well as their counterintuitive physical properties in the quantum domain [1, 2].

Quasi-particle current flows across an open mesoscopic ring connected to electron reservoirs via leads maintained at a constant chemical potential difference. The current I injected by the reservoir into one of the leads splits into I_U and I_L in the upper and lower arms of the ring such that current conservation (Kirchoff's law : $I = I_U + I_L$) is satisfied. The size of the ring being smaller than the phase coherence length, the electrons in two arms in general will pick up different phases and their quantum mechanical superposition gives rise to two distinct possibilities. The first being, for some values of Fermi energy the currents in the two arms I_U and I_L are individually less than the total current I , i.e., the current in both arms

flow along the direction of the applied field. The other possibility is that for some values of Fermi energy, I_U (or I_L) can be greater than the total current I . In this case current conservation dictates I_L (or I_U) to be negative such that $I = I_L + I_U$. The property that the current in one of the arms is larger than the transport current is referred to as ‘**current magnification**’ effect [3, 4, 5]. Magnitude of this negative current is taken to be that of the ‘circulating current’. When negative current flows in the upper arm the direction of the circulating current is taken to be counter clockwise or negative and when it flows in the lower arm its direction is taken to be clockwise or positive. It should be noted that these circulating currents arise in the absence of magnetic flux, but in the presence of transport current (i.e., in a nonequilibrium system). When a parallel resonance circuit (capacitance C connected in parallel with a combination of inductance L and resistance R) is driven by an external e.m.f., circulating current arises in the circuit at resonance frequency [6]. However, the current magnification effect is absent in a circuit with two parallel resistors in the presence of dc current in the classical regime. In a mesoscopic ring the intrinsic wave nature of electrons and their phase coherence gives rise to this effect even in presence of dc driving voltage. Studies on current magnification effect in mesoscopic open rings have been extended to thermal currents [7] and to spin currents in presence of Aharonov-Casher flux [8]. This effect has been studied in the presence of

*Electronic address: swarnali@bose.res.in

†Electronic address: deo@bose.res.in

‡Electronic address: jayan@iopb.res.in

a spin-flip scatterer which causes dephasing of electronic motion [9, 10].

The predicted magnitude of the circulating current densities can indeed be very large [4] and has been termed as ‘giant persistent currents’ [11, 12]. Recently the current magnification effect has been shown to occur in mesoscopic hybrid system at equilibrium in the presence of a magnetic flux and in the absence of transport current [13, 14]. So far all studies on current magnification have been restricted to the case of one dimensional (single channel) systems only. In this work we go beyond the single channel regime to a multi-channel one. Multi-channel systems are a closer realisation to the experimental systems [15, 16] due to their finite width in the transverse direction of propagation of currents. In the present work we show that inspite of the contributions from large number of different modes and mode-mixing, current magnification sustains for various length ratios of the two arms of the ring. The connection between current magnification and Fano resonance in the total current is shown. In very special cases current magnification is shown to occur near Briet-Wigner type resonances. The strong qualitative dependence of current magnification and system-reservoir coupling strength is also established.

II. DESCRIPTION OF THE SYSTEM

In our present work we consider a quasi-one-dimensional (Q1D) ring of perimeter L and width W with $L \gg W$ as shown in Fig. 1. The two leads that connect this system to the electron reservoirs have the same width as that of the ring. The length of the lower arm of the ring is l_3 while that of the upper arm is $l_1 + l_2$. An impurity δ function potential $V\delta(x - l_1)\delta(y - y_i)$ is embedded in the upper arm. The electrons can propagate freely along the length of the ring and leads but their motion is confined along the transverse direction. We consider hard wall confinement potential along the transverse direction. Due to this confinement, infinite number of transverse modes are generated in the system. If the energy of the electrons is such that the corresponding wave number is real then the mode is termed as propagating, on the other hand, if the wave number

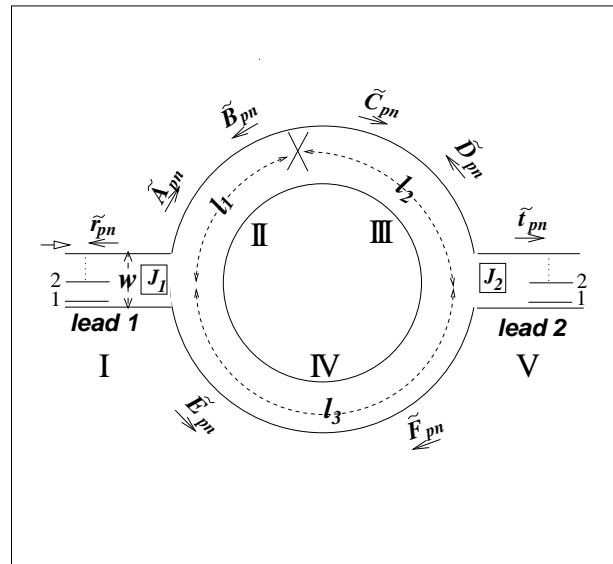


FIG. 1: Schematic diagram of an open multi-channel mesoscopic ring of perimeter $L = l_1 + l_2 + l_3$ connected through the leads 1 and 2 to electron reservoirs (not shown in figure). Both the ring and the leads have the same width W . Several transverse modes are shown by horizontal lines in the leads. A delta function type static scatterer $V_d(x, y) = V\delta(x - l_1)\delta(y - y_i)$ of strength V is shown in the upper arm at \times . ϵ denotes the coupling strength between leads and the ring.

is imaginary it is termed as evanescent. The widths of the ring and leads being equal the number of propagating and evanescent modes are same in these two.

We consider the non-interacting electrons in the system. The system size is taken to be smaller than the phase coherence length l_ϕ and the phase randomizing inelastic scattering is considered only inside the reservoir. Scattering inside the system maintains the phase coherence. This necessitates only static scatterers in the system which in our case are a delta-function potential and junction scatterers at $J1$ and $J2$. We neglect all phase randomizing scattering like electron-phonon interaction inside the system. The left reservoir (R_L) and the right reservoir (R_R) have chemical potentials μ_L and μ_R respectively. When $\mu_L > \mu_R$ current flows from R_L to R_R and vice-versa. We are interested in the linear response regime where currents are related to the transmission across the system at the Fermi energy (Landauer-Büttiker formula, [1]). We consider that the electrons enter the system through the left lead and come out through the right lead. Due to mirror symmetry, results remain

the same if the flow of electrons is reversed with the direction of circulating current getting reversed. This ensures absence of circulating current in equilibrium at zero magnetic field. Magnetic field breaks the time reversal symmetry and hence one can obtain persistent currents circulating across the ring in equilibrium [17]. These currents have been observed experimentally both in open and closed systems [2, 18].

For no loss of generality we have considered the situation wherein no mode mixing between different transverse modes occur at the junctions. The ring and the lead are connected via junction scattering matrices at $J1$ and $J2$. The junction scattering matrices are same for both the junctions $J1$ and $J2$. The coupling between either sides of the junction for the modes with same transverse quantum number is given by [19]

$$S_J = \begin{pmatrix} -(a+b) & \sqrt{\epsilon} & \sqrt{\epsilon} \\ \sqrt{\epsilon} & a & b \\ \sqrt{\epsilon} & b & a \end{pmatrix} \quad (1)$$

where $a = \frac{1}{2}(\sqrt{1-2\epsilon}-1)$ and $b = \frac{1}{2}(\sqrt{1-2\epsilon}+1)$. ϵ is a coupling parameter with values $0 \leq \epsilon \leq 0.5$. When $\epsilon \rightarrow 0$ the system and the reservoir are decoupled while for $\epsilon \rightarrow 0.5$ these two are strongly coupled. This S -matrix satisfies the conservation of current [20]. The above S -matrix is independent of the incident energy and the index of the transverse modes. The presence of the elastic scatterer, namely, δ function potential in the upper arm mixes different propagating and evanescent modes along with extra phase shift in the same mode.

When electrons are injected in the p -th propagating mode, the total wave function in the left lead (region I) is given by

$$\psi|_{\text{I}} = \sqrt{N}e^{ik_p x}\chi_p(y) + \sum_n r_{pn}e^{-ik_n x}\chi_n(y), \quad (2)$$

where k_p is the longitudinal wavevector corresponding to p -th mode along the direction of propagation. Here r_{pn} describes reflection amplitude from p -th mode to n -th mode, $\chi_n(y)$ represents the n th transverse mode where y is the coordinate along the transverse direction and \sum_n denotes summation over n including p . The normalisation factor \sqrt{N} is determined by noting that the current density injected by the reservoir in a small energy interval dE in the p -th propagating mode is

$$dj_{p_{in}} = ev_p \frac{dn_p}{dE} f(E) dE \quad (3)$$

where $f(E)$ is the Fermi distribution function, $\frac{dn_p}{dE} = \frac{2}{\hbar v_p}$ is the density of states (DOS) in the perfect wire and $v_p = \frac{\hbar k_p}{m_e}$. For our zero temperature calculations $f(E) = 1$ for occupied states. The wave function $\psi_p|_{\text{I}}$ gives the incident current density $dj_{p_{in}} = \frac{2e}{\hbar} dE$, which in turn is independent of the propagating mode in which the electron is incident if $N = \frac{2e}{\hbar v_p} dE$. Here dE denotes an energy interval around Fermi energy and hence change in incident energy would mean a change in the Fermi energy of electrons emanating from the reservoirs.

The wave functions in all other regions are

$$\psi|_{\text{II}} = \sum_n (A_{pn}e^{ik_n x} + B_{pn}e^{-ik_n x})\chi_n(y) \quad (4)$$

$$\psi|_{\text{III}} = \sum_n (C_{pn}e^{ik_n x} + D_{pn}e^{-ik_n x})\chi_n(y) \quad (5)$$

$$\psi|_{\text{IV}} = \sum_n (E_{pn}e^{ik_n x} + F_{pn}e^{-ik_n x})\chi_n(y) \quad (6)$$

$$\psi|_{\text{V}} = \sum_n t_{pn}e^{ik_n x}\chi_n(y) \quad (7)$$

where n stands for all available propagating modes including p .

S_J connects the incoming and outgoing amplitudes of the p -th mode at J_1 via

$$\begin{pmatrix} \tilde{r}_{pp} \\ \tilde{A}_{pp} \\ \tilde{E}_{pp} \end{pmatrix} = S_J \begin{pmatrix} 1 \\ \tilde{B}_{pp} \\ \tilde{F}_{pp} \end{pmatrix} \quad (8)$$

where any new amplitude \tilde{A}_{pn} is connected to its earlier definition A_{pn} by

$$\tilde{A}_{pn} = \sqrt{v_p} \sqrt{\frac{\hbar}{2e}} (\sqrt{dE})^{-1} A_{pn}$$

In further calculations all the tilded amplitudes carry the same meaning as above. S_J connects the incoming and outgoing amplitudes of all the other propagating modes m ($m \neq p$) at J_1 via

$$\begin{pmatrix} \tilde{r}_{pm} \\ \tilde{A}_{pm} \\ \tilde{E}_{pm} \end{pmatrix} = S_J \begin{pmatrix} 0 \\ \tilde{B}_{pm} \\ \tilde{F}_{pm} \end{pmatrix} \quad (9)$$

Similarly, the incoming amplitudes ($0, \tilde{C}_{pn}, \tilde{E}_{pn}$) and outgoing amplitudes ($\tilde{t}_{pn}, \tilde{D}_{pn}, \tilde{F}_{pn}$) at the junction J_2 are connected via the same scattering matrix S_J .

The elastic scattering at the impurity is described by

$$\begin{pmatrix} \tilde{B}_{p1} e^{-ik_1 l_1} \\ \tilde{B}_{p2} e^{-ik_2 l_1} \\ \dots \\ \dots \\ \tilde{B}_{pP} e^{-ik_P l_1} \\ \tilde{C}_{p1} \\ \tilde{C}_{p2} \\ \dots \\ \dots \\ \tilde{C}_{pP} \end{pmatrix} = \tilde{S} \begin{pmatrix} \tilde{A}_{p1} e^{ik_1 l_1} \\ \tilde{A}_{p2} e^{ik_2 l_1} \\ \dots \\ \dots \\ \tilde{A}_{pP} e^{ik_P l_1} \\ \tilde{D}_{p1} \\ \tilde{D}_{p2} \\ \dots \\ \dots \\ \tilde{D}_{pP} \end{pmatrix} \quad (10)$$

$$\text{where } \tilde{S} = \begin{pmatrix} \tilde{R} & \tilde{T} \\ \tilde{T} & \tilde{R} \end{pmatrix}$$

and both \tilde{R} and \tilde{T} are matrices of order $P \times P$, P being the maximum number of propagating modes in the system depending on a given Fermi energy. Here

$$\tilde{R} = \begin{pmatrix} \tilde{\rho}_{11} & \tilde{\rho}_{12} & \dots & \dots & \tilde{\rho}_{1P} \\ \tilde{\rho}_{21} & \tilde{\rho}_{22} & \dots & \dots & \tilde{\rho}_{2P} \\ \dots & \dots & \dots & \dots & \dots \\ \dots & \dots & \dots & \dots & \dots \\ \tilde{\rho}_{1P} & \tilde{\rho}_{2P} & \dots & \dots & \tilde{\rho}_{PP} \end{pmatrix}$$

and

$$\tilde{T} = \begin{pmatrix} \tilde{\tau}_{11} & \tilde{\tau}_{12} & \dots & \dots & \tilde{\tau}_{1P} \\ \tilde{\tau}_{21} & \tilde{\tau}_{22} & \dots & \dots & \tilde{\tau}_{2P} \\ \dots & \dots & \dots & \dots & \dots \\ \dots & \dots & \dots & \dots & \dots \\ \tilde{\tau}_{1P} & \tilde{\tau}_{2P} & \dots & \dots & \tilde{\tau}_{PP} \end{pmatrix},$$

$$\text{where } \tilde{\rho}_{mn} = \frac{-i \frac{\Gamma_{mn}}{2\sqrt{k_m k_n}}}{1 + \sum_j^e \frac{\Gamma_{jj}}{2k_j} + i \sum_j^p \frac{\Gamma_{jj}}{2k_j}}.$$

\sum^e represents sum over all the evanescent modes and \sum^p represents sum over all the propagating modes and the modes m and n are assumed as propagating. The intermode (i.e. $m \neq n$) transmission amplitudes are $\tilde{\tau}_{mn} = \tilde{\rho}_{mn}$ and intramode transmission amplitudes are $\tilde{\tau}_{nn} = 1 + \tilde{\rho}_{nn}$. For details see Ref.[21]. Γ_{mn} can be calculated using

$$\Gamma_{mn} = \frac{2m_e V}{\hbar^2} \chi_n^*(y_i) \chi_m(y_i).$$

In Eq. 10, while writing \tilde{A}_{pn} , \tilde{B}_{pn} the origin is taken to be at the junction J_1 whereas in writing \tilde{C}_{pn} , \tilde{D}_{pn} the

origin is taken at the scatterer. For details of the S -matrix elements for a multi-channel scattering problem see Ref. [21]. Note that different elements of the S -matrix contains information about the propagating modes as well as all the infinite number of evanescent modes arising out of transverse confinement [21].

For any given incident electron in the p -th mode in the lead with energy E the current in the n -th mode in region II is given by

$$\begin{aligned} dj_{p,n_{LU}} &= v_n (|A_{pn}|^2 - |B_{pn}|^2) \\ &= (|\tilde{A}_{pn}|^2 - |\tilde{B}_{pn}|^2) \frac{2e}{h} \end{aligned} \quad (11)$$

Currents in all other portions of the ring can be calculated similarly. The partial current densities $dj_{p,n_{LU}}$ are obtained after integrating the local currents along the transverse y direction. If $dj_{p,n}$ is the current density in the n -th propagating mode in any segment of the system then the total current in that segment is given by

$$dj = \sum_{p=1}^P dj_p(s) = \sum_{p=1}^P \sum_{n=1}^P dj_{p,n} \quad (12)$$

where ‘ p ’ denotes the propagating mode in which the electrons are injected from the reservoir.

We use scattering matrices at the two junctions and at the scatterer site, \times , to calculate all the amplitudes and then find out the total current density (dj_T), the current density in the upper arm (dj_U) as well as in the lower arm (dj_L). Thus

$$\begin{aligned} dj_T &= \sum_{p=1}^P \sum_{n=1}^P |\tilde{t}_{pn}|^2 \frac{2e}{h} \\ &= \sum_{p=1}^P \left(1 - \sum_{n=1}^P |\tilde{r}_{pn}|^2\right) \frac{2e}{h} \end{aligned} \quad (13)$$

We study these currents as a function of the incident electron energies.

III. RESULTS AND DISCUSSIONS

The circulating current density dj_c is the magnitude of the negative part of dj_U or dj_L as mentioned earlier. When dj_U is negative the direction of circulating electron current is anticlockwise (negative) and when dj_L is negative then it is clockwise (positive). A circulating current

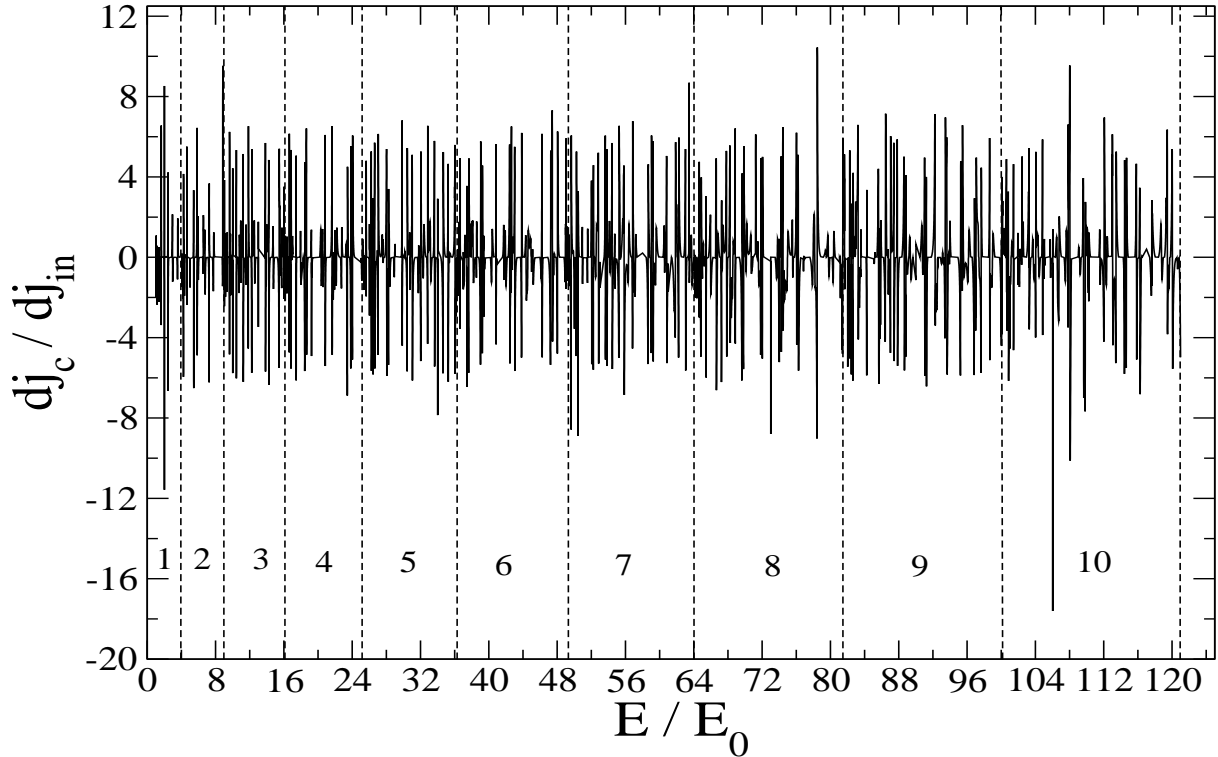


FIG. 2: Plot of circulating current density dj_c/dj_{in} in the ring as a function of E/E_0 of the electron. In the whole energy range, we have 1 to 10 propagating modes (corresponding energy-range are indicated by vertical dashed lines). The different system parameters are $l_1 = 3.5$, $l_2 = 2.5$, $l_3 = 4.0$, $W = 1$, $V = 1$, $y_i = 0.21W$, $\epsilon = 0.2$.

in a loop gives rise to an orbital magnetic moment (Ampere's law). By our convention, positive dj_c indicates an 'up' magnetic moment whereas negative dj_c indicates a 'down' one. We plot all current densities in units of incident current density $dj_{in} = \frac{2e}{h}dE$ and all energies in units of ground state energy of the lowest transverse mode, $E_0 = \frac{\pi^2 \hbar^2}{2m_e W^2}$. In all our calculations we have considered 500 evanescent modes. Increasing the strength of the impurity potential causes the coupling of higher number of evanescent modes and hence for large impurity potential strengths one need to incorporate larger number of evanescent modes.

We first study the case for which the system is weakly coupled with the leads (Fig. 2). This coupling can be controlled by appropriately changing the values of ϵ . All the physical parameters are indicated in the figure caption. The upper and lower arms of the ring have different lengths. From the plot of circulating current density vs. energy (Fig. 2) we observe that there is current magnification of almost same magnitude with similar frequency

of occurrence over the entire energy range. The total number of propagating modes in the lead incident on the ring vary throughout this energy scale from one to ten as indicated in Fig. 2. Number of propagating modes in the lead and the ring are same. Between different propagating modes there are several resonances around which current magnification takes place [3, 4]. These resonances approximately occur around $E_r = \hbar^2 \left(\frac{2r\pi}{L}\right)^2$, where E_r is the energy eigenvalues of the isolated ring of length L . The small deviations of resonances from these values is due to multi-channel nature of our problem along with impurity potential which causes mode mixing. When there are say ten propagating modes, to obtain total current in the upper arm we have to add hundred values of partial currents [Eq. 12] due to different modes. Though individual partial current density show oscillatory behaviour the magnitude of the total circulating current remains of the same order when there is only one propagating mode in the system. This can be explicitly seen in Fig. 2 throughout the energy range

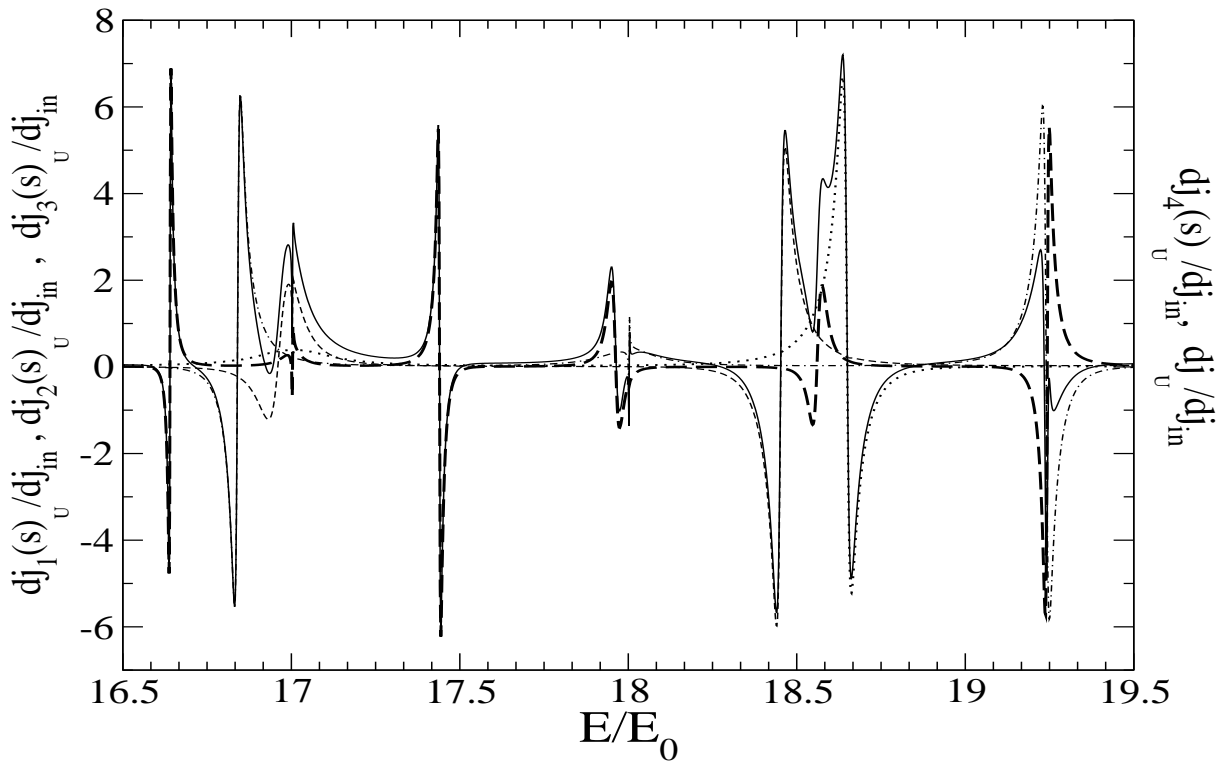


FIG. 3: Plots of different partial current densities and the total current in the upper arm of the ring as a function of E/E_0 . The dotted curve gives $dj_1(s)_U/dj_{in}$, the dashed curve gives $dj_2(s)_U/dj_{in}$, the dash-dotted curve gives $dj_3(s)_U/dj_{in}$, the long-dashed one is for $dj_4(s)_U/dj_{in}$ and the solid one is for dj_U/dj_{in} . In the above energy range we have 4 propagating modes. The different system parameters are $l_1 = 3.5$, $l_2 = 2.5$, $l_3 = 4.0$, $W = 1$, $V = 1$, $y_i = 0.21W$, $\epsilon = 0.2$.

with one to ten propagating modes. This clearly indicates that current magnification effect is robust even in multi-channel systems inspite of contributions from several propagating modes and mode mixing. To see the mode mixing and the cancellation effects we have considered the case where there are four propagating modes in Fig. 3. Hence to obtain total current in the upper arm we have to calculate sixteen partial currents [Eq.12]. In Fig. 3, for simplicity instead of considering sixteen partial currents we have plotted four values of current densities $dj_1(s)_U, dj_2(s)_U, dj_3(s)_U, dj_4(s)_U$ and total current dj_U . Here $dj_i(s)_U = \sum_{n=1}^4 dj_{i,n}$, $i = 1, 2, 3, 4$. $dj_{i,n}$ is sum over partial current densities in the four propagating modes in the upper arm when electron is incident in the i -th propagating mode. Total current in the upper arm is given by $dj_U = dj_1(s)_U + dj_2(s)_U + dj_3(s)_U + dj_4(s)_U$. Negative currents in this graph represents the existence of circulating current in partial current densities. Each $dj_i(s)_U$ show oscillatory and complex pattern. The total

current dj_U still exhibits negative part (current magnification) inspite of cancellation effects arising due to mode mixing.

To see in detail the nature of current magnification vis-a-vis total transport current in lead we consider a case where there is only one propagating mode (Fig. 4(a)) and separately another case wherein number of propagating modes are ten (Fig. 4(b)). In these figures we have plotted the total transport current and circulating currents as a function of Fermi energy with the other parameters are mentioned in figure caption. We see a current magnification whenever there is a partial minimum in the total current that flows through the system which in turn is measured at the leads. This is consistent with earlier observations seen in the case of one dimensional system [3].

When only one channel is propagating the total current is proportional to the transmission coefficient [1]. A closer look at these minima shows that we obtain cur-

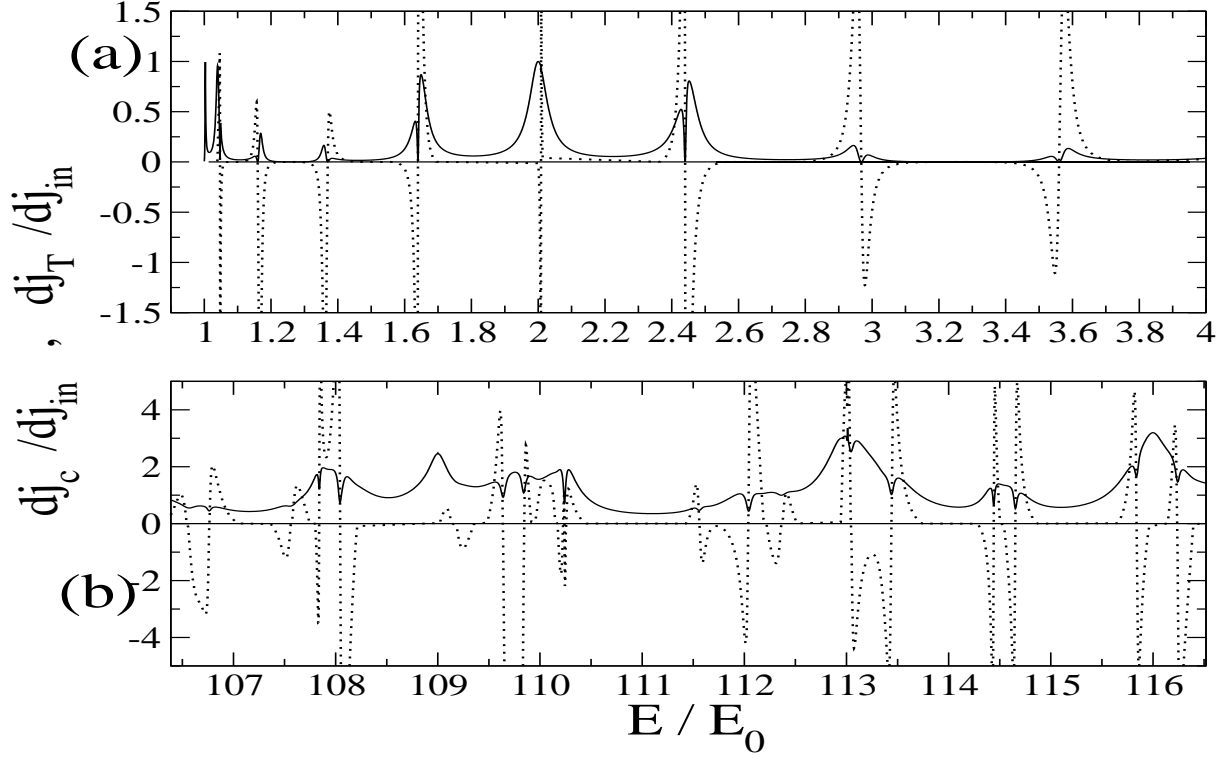


FIG. 4: Plot of the circulating current dj_c/dj_{in} (dotted lines) and the total current dj_T/dj_{in} (solid lines). Both the functions are plotted versus E/E_0 . The different system parameters are $l_1 = 3.5$, $l_2 = 2.5$, $l_3 = 4.0$, $W = 1$, $V = 1$, $y_i = 0.21W$, $\epsilon = 0.2$.

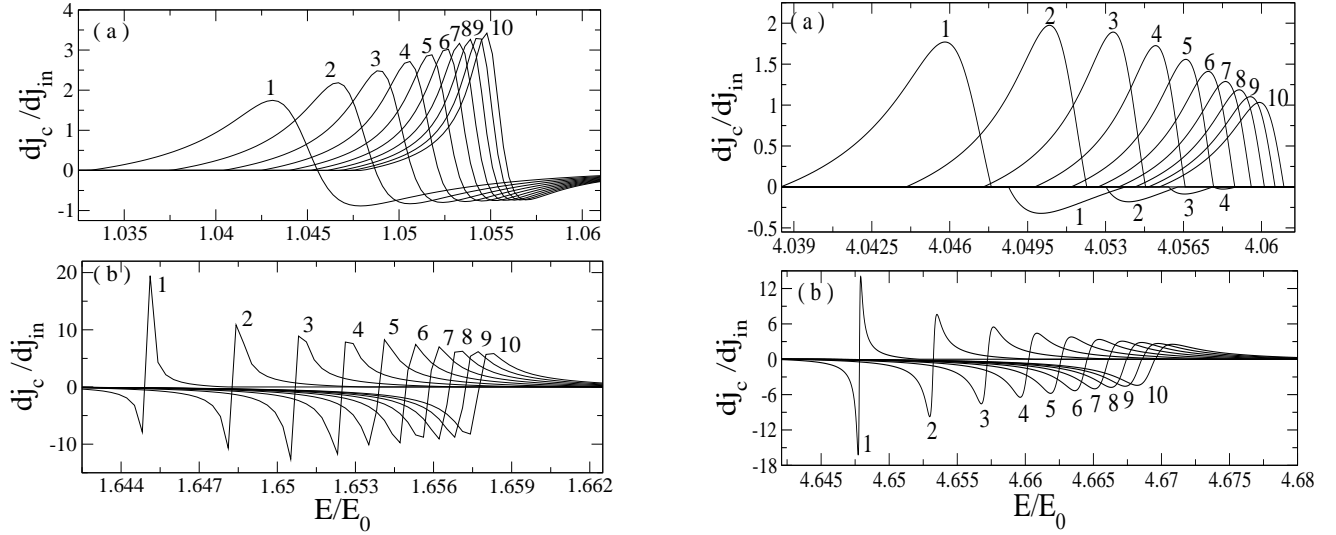


FIG. 5: Plots of circulating current dj_c/dj_{in} versus incident energy E/E_0 in the range of single mode propagation. Curves 1, 2, 3, 4, \dots , 10 are for potential strengths $V = 0.5, 1.0, 1.5, 2.0, \dots, 5.0$ respectively. The other system parameters are $l_1 = 3.125$, $l_2 = 3.125$, $l_3 = 3.75$, $W = 1$, $y_i = 0.21W$, $\epsilon = 4/9$.

FIG. 6: Plots of circulating current dj_c/dj_{in} versus incident energy E/E_0 in the range of two mode propagation. Curves 1, 2, 3, 4, \dots , 10 represent potential strengths $V = 0.5, 1.0, 1.5, 2.0, \dots, 5.0$ respectively. The other system parameters are $l_1 = 3.125$, $l_2 = 3.125$, $l_3 = 3.75$, $W = 1$, $y_i = 0.21W$, $\epsilon = 4/9$.

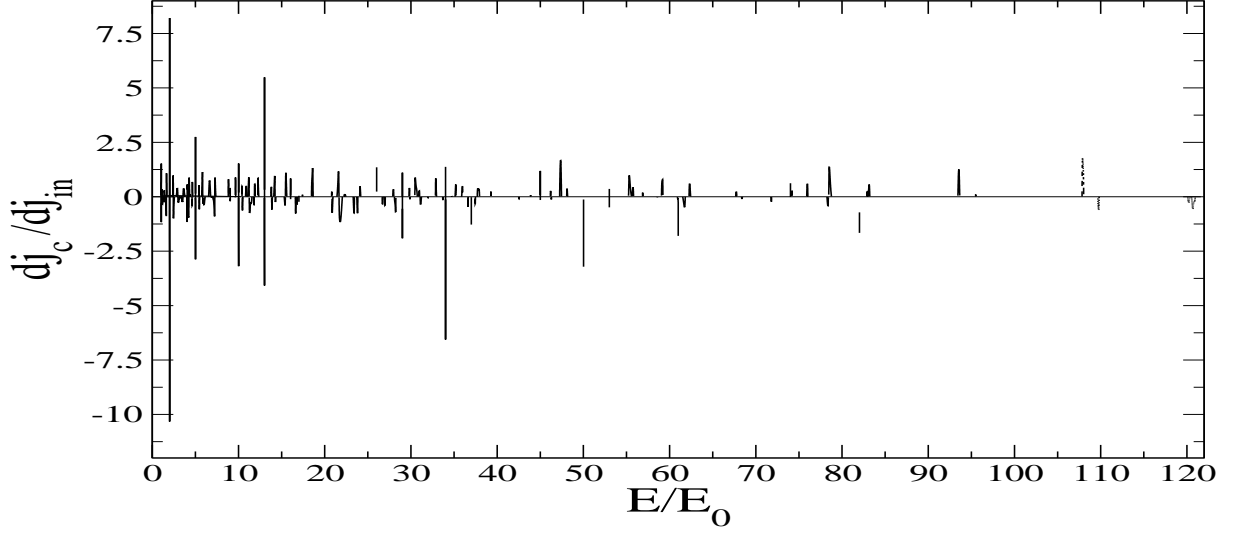


FIG. 7: The circulating current dj_c/dj_{in} versus E/E_0 is plotted for repulsive potential $V = 1$ in strong coupling regime $\epsilon = 0.48$. The different system parameters are $l_1 = 3.5$, $l_2 = 2.5$, $l_3 = 4.0$, $W = 1$, $y_i = 0.21W$.

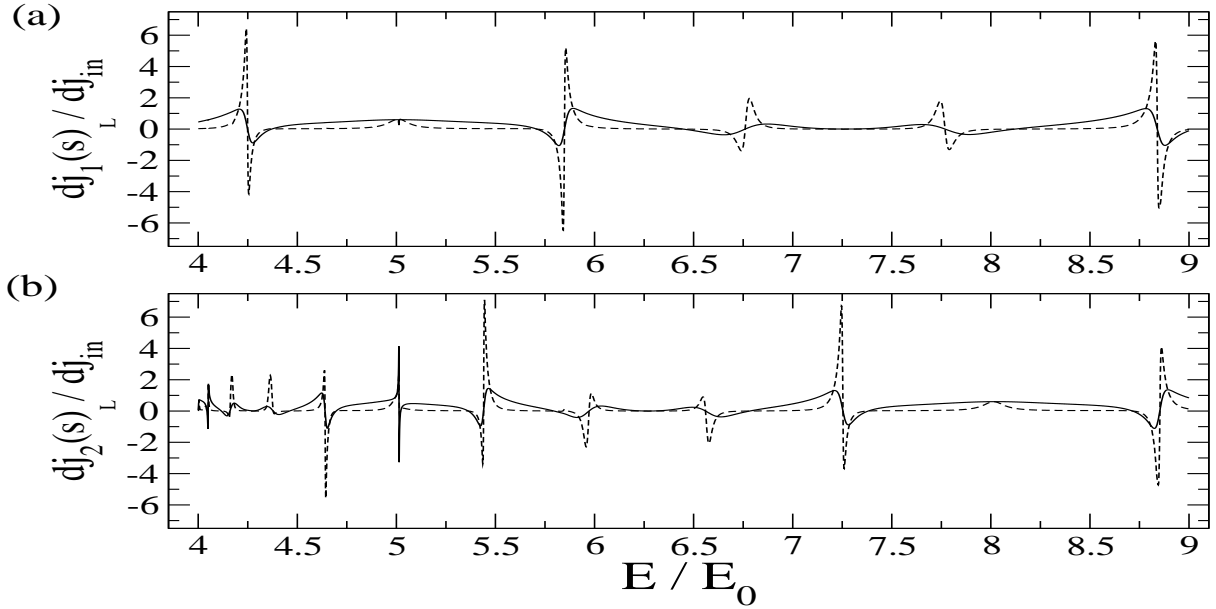


FIG. 8: In (a) the partial current $dj_1(s)_L/dj_{in}$ and in (b) the partial current $dj_2(s)_L/dj_{in}$ in the lower arm of the ring are plotted as a function of E/E_0 . In both (a) and (b) dashed curves are for $\epsilon = 0.2$ and the solid curves are for $\epsilon = 0.48$. The other system parameters are $l_1 = 3.5$, $l_2 = 2.5$, $l_3 = 4.0$, $W = 1$, $V = 1$, $y_i = 0.21W$.

rent magnification of either sign around every maxima-minima pair in total current. In Ref. [3, 11, 12] the current magnification of a pure 1D quantum ring having no impurity has been related to Fano resonance (asymmetric zero-pole structure) in the transmission co-

efficient. In multi-channel transmission Fano zero-pole line shape gets replaced by an asymmetric maximum-minimum lineshape [22]. We found this Fano type asymmetric maxima-minima lineshape at each energy point of current magnification shown in Fig. 2. From a first

look in the range $1.8E_0 < E < 2.2E_0$ in Fig. 4(a) it appears that we have current magnification near a total-current maximum. But a closer scan reveals that there is indeed a very sharp Fano-type asymmetric maxima-minima lineshape at this point, though it is not visible in the graph. At current magnification the presence of a quasi-bound state of circulating current in the ring gives rise to this Fano-type lineshape to the total current. The circulating current changes sign more sharply and shows stronger current magnification where Fano lineshape is sharper and narrower. This feature is somewhat equivalent to the classical parallel LCR resonance circuit in which the higher Q -values indicate higher current magnification and sharper minimum at resonant frequencies. These features remain intact for whole energy scale even if there are more than one propagating modes contributing (see Fig. 4(b)).

We observe that for a symmetric ring ($l_1 + l_2 = l_3$) frequency of the occurrence of current magnification reduces throughout this energy scale considered earlier. This is understandable as in the absence of any impurity and magnetic field an asymmetric 1D ring shows current magnification [3], meaning that asymmetry in length ratios of

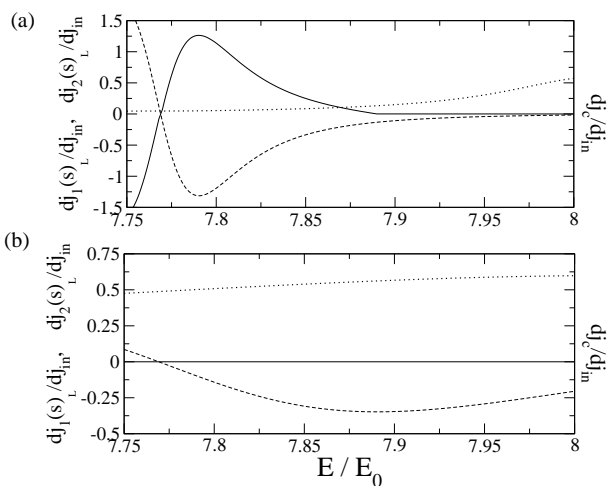


FIG. 9: Both in (a) and (b), the dashed curve gives the partial current $dj_1(s)_L/dj_{in}$, the dotted curve gives the partial current $dj_2(s)_L/dj_{in}$ in the lower arm of the ring and the solid curve gives the circulating current dj_c/dj_{in} in the ring. All three functions are plotted as a function of incident energy E/E_0 of the electron. (a) is for weak coupling $\epsilon = 0.2$ while (b) is for strong coupling $\epsilon = 0.48$. Other system parameters are $l_1 = 3.5$, $l_2 = 2.5$, $l_3 = 4.0$, $W = 1$, $V = 1$, $y_i = 0.21W$.

a ring favours this effect. Pareek *et al.* [4] have shown that for a 1D ring one can have regions of incident energies where current magnification gets enhanced with the increase in the impurity potential strength. We investigate this effect for the case of our multi-channel ring. In order to compare with Ref. [4] we have calculated the effects of potential using Griffiths boundary condition or coupling parameter $\epsilon = 4/9$ at the junctions. In Fig. 5 and Fig. 6 we have shown the variation of the current magnification for two different peaks in the appropriate energy ranges. The Fig. 5 is for single channel case while Fig. 6 is for two channel. From Fig. 5(a) and Fig. 6(a) we notice that the current magnification effect get enhanced with the increase in strength of the impurity potential while the opposite is true for the case considered in Fig. 6(b). A closer look at Fig. 5(b) reveals that peak in the negative part of the circulating current density first increases and then decreases as we vary continuously the strength of the impurity potential. Thus impurities in the system can either enhance or decrease the current magnification effect. The enhancement of the circulating current densities is a counter-intuitive effect, in the light of the fact that impurity generally degrades the transport current in the system.

Büttiker [19] has shown that when the ring is threaded by a magnetic flux Φ , as the coupling goes towards the strong coupling regime ($\epsilon \rightarrow 0.5$) the amplitude of persistent current reduces due to increased dephasing. This is a quantitative change in persistent current due to broadening of energy levels with increasing coupling strength. To examine the effect of system-reservoir coupling strength on current magnification in multi-channel ring in absence of Φ , we have calculated circulating current for $\epsilon = 0.48$. We observe that the frequency of current magnification as well as the magnitude of circulating currents reduce significantly in the whole energy range (Fig. 7) compared to that observed in Fig. 2. This indicates that in Q1D coupling strength alters the nature of current magnification effect in a non-trivial manner. The total current magnification in the ring is due to a summation over current magnifications corresponding to each incident mode allowed for a given incident energy. As we increase the coupling strength ϵ , we observe that the contribution to current magnification from electrons injected in each incident mode goes from a narrower and stronger

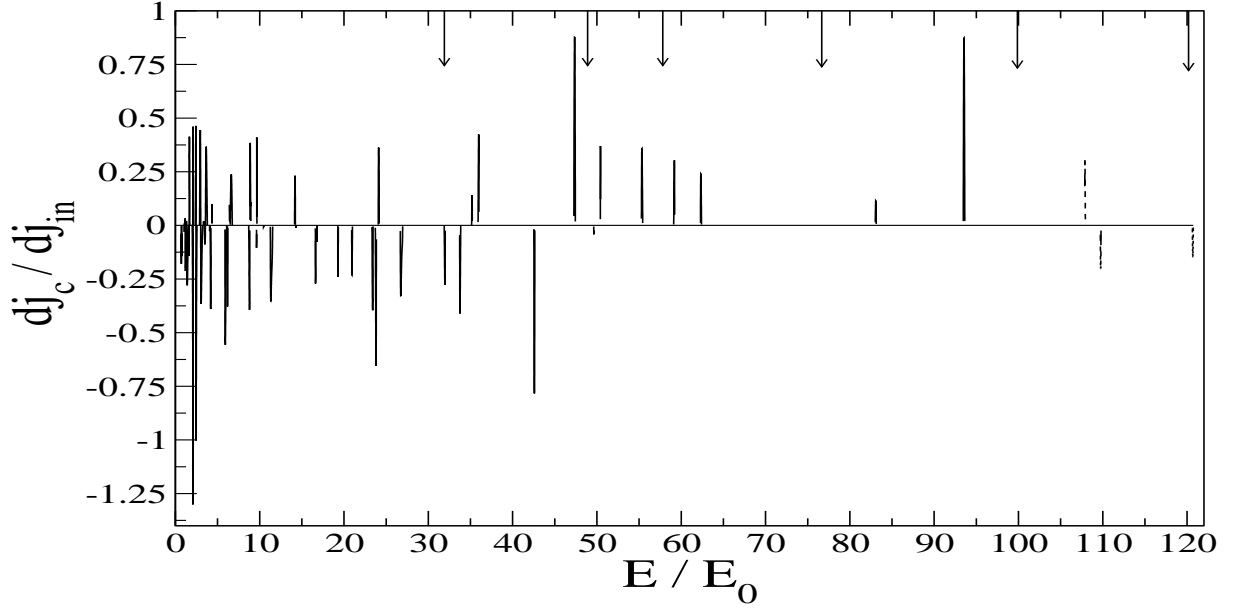


FIG. 10: The circulating current dj_c/dj_{in} vs. E/E_0 is plotted for strong coupling $\epsilon = 0.48$ and attractive potential $V = -2.5$. The arrows on the graph denotes the positions of different quasi-bound-states in the available energy range, $31.87 E_0, 49 E_0, 57.7 E_0, 76.53 E_0, 100 E_0, 120.12 E_0$. The other system parameters are $l_1 = 3.5, l_2 = 2.5, l_3 = 4.0, W = 1, y_i = 0.21W$.

to a broader and weaker shape with respect to the corresponding energies (Fig 8). The more broader they get, the more cancellation of current magnification occurs due to overlap of different incident modes. In Fig. 9 we have shown contributions from first and second incident modes

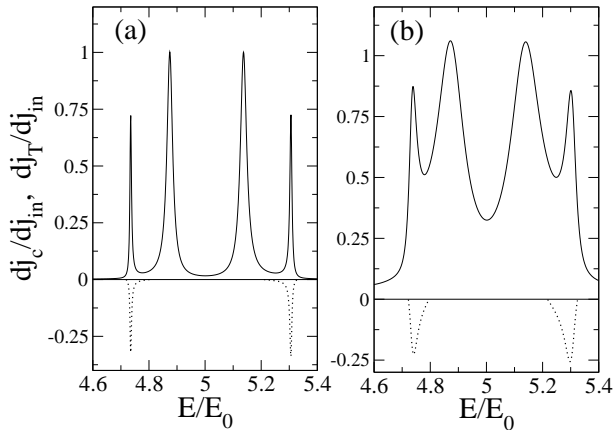


FIG. 11: dj_T/dj_{in} (solid curve) and dj_c/dj_{in} (dotted curve) are plotted as a function of E/E_0 for coupling strengths(ϵ) 0.05 ((a)) and 0.2 ((b)) in presence of two propagating modes. Other system parameters are $V = -2.4, l_1 = 2.5, l_2 = 1.5, l_3 = 3.0, W = 1, y_i = 0.21W$. The quasi-bound-state is at $5.1025E_0$.

in the upper arm of the ring when only two modes are propagating. In this energy range we observe current magnification for $\epsilon = 0.2$ (upper graph) and no current magnification for $\epsilon = 0.48$ (lower graph). From lower graph ($\epsilon = 0.48$) it is evident that though the contribution of current due to incident mode-1 (dashed line) is negative and thus should give rise to current magnification, the contribution from incident mode-2 (dotted line) cancels it off and we observe no net current magnification in this energy range. From the upper graph ($\epsilon = 0.2$) it is clear that in the energy range where contribution of current due to incident mode-1 (dashed line) is negative, the contribution from incident mode-2 (dotted line) is almost zero as the contribution to current magnification from each incident mode is very sharp for low ϵ -values. Hence we obtain a net current magnification in this energy range for $\epsilon = 0.2$ though current magnification is absent for $\epsilon = 0.48$ in the same energy range. Thus system-reservoir coupling strength alters current magnification effect in a multi-channel mesoscopic ring not only quantitatively, but it also has a strong qualitative effect. The stronger the coupling the weaker and lesser is the current magnification in any energy scale. As for energies where higher number of modes are propagating

and number of cancellations of current magnification is also high we obtained even less current magnifications and their occurrence frequency in the energy axis are also reduced (Fig. 7). This effect is entirely due to the superposition of currents from all the different channels which is absent in purely 1D system. The non-trivial effect of system-reservoir coupling on the equilibrium currents in 1D quantum double ring system has been discussed recently in Ref.[23].

We now consider the case of an attractive impurity δ function potential ($V < 0$). We see in Fig. 10 that the amplitude of current magnification is lesser in the stronger coupling regime ($\epsilon = 0.48$) in comparison to Fig. 7. The magnitude and positions of the current peaks are very sensitive to the details of the system parameters and they can not be predicted a priori. Moreover, the current magnification effect is always absent at the quasi-bound state of the negative potential (Fig. 10). The energies of the quasi-bound states are marked by arrows in Fig. 10. Quasi-bound states are characterised by peak in the density of states (DOS) and for further discussion on quasi-bound state see Ref. [21, 22, 24]. The presence of negative delta-function potential enhances DOS near this potential. This enhanced local DOS at the impurity site reduces the DOS of the propagating electrons thereby reducing the current magnification.

In Fig. 11 we have considered a special case and plotted the total transport current density dj_T and circulating current density dj_c in the energy range $4.6E_0 < E < 5.4E_0$. In this energy range at the Fermi energy there are two propagating modes. The corresponding bound-state is at $5.1025E_0$. Around the bound-state there is an enhancement in scattering. The structure of the total transport current exhibits a symmetric line shapes (like Briet-Wigner type symmetric resonances). Around these resonances we do observe current magnification. This special case shows that Fano type resonance structure in the total transport current is not a necessary criteria for the observation of current magnification effect.

IV. CONCLUSION

In conclusion, we have shown that for a system weakly coupled with reservoirs current magnification is a robust

effect even in multi-channel case in the presence of transport current. The magnitude of the circulating current can be very large even in presence of several propagating modes despite mode mixing and cancellation effects as discussed in the text. The circulating current are mostly associated with Fano resonance in total transport current. However, there are sometimes exception to this rule, namely, current magnification may occur around Briet-Wigner type symmetric resonances in the total current. Unlike purely one dimensional system Fano resonance does not exhibit the zero in the total transmission, however, it is characterised by a sharp minimum along with asymmetric line shapes in the total current. Impurity strength can enhance or suppress current magnification and is sensitively dependent on system parameters. We have established that the system-reservoir coupling strength controls the current magnification qualitatively. As the coupling becomes stronger the current magnification becomes weaker and its occurrence in the given energy range reduces. Thus system reservoir coupling parameter controls the transport properties in a very interesting manner. It is interesting to note that persistent currents in a ballistic mesoscopic ring in the presence of magnetic flux increases with the Fermi energy (or the number of channels) [25]. In contrast the magnitude of the current magnification is independent of the total number of propagating channels. It may be emphasized that persistent currents and the circulating currents due to current magnification are two independent distinct phenomena [26].

V. ACKNOWLEDGMENTS

One of the authors (S.B.) thanks Prof. Binayak Dutta Roy, Debasish Chaudhuri and Raishma Krishnan for several useful discussions. S.B. also thanks Institute of Physics, Bhubaneswar for providing local hospitality where part of the work was carried out.

-
- [1] S. Datta, *Electronic Transport in Mesoscopic Systems*, Cambridge University Press, Cambridge, UK, (1997).
- [2] Y. Imry, *Introduction to Mesoscopic Physics*, Oxford University Press, 1997.
- [3] A. M. Jayannavar and P. Singha Deo , Phys. Rev. B **51**, 10175 (1994).
- [4] T. P. Pareek , P. Singha Deo and A. M. Jayannavar , Phys. Rev. B **52**, 14657 (1995).
- [5] A. M. Jayannavar , P. Singha Deo and T. P. Pareek , Physica B **212**, 216 (1995).
- [6] D.F.Shaw, *An Introduction to Electronics*, 2nd ed., (Longman, London, 1970), p. 51.
- [7] M.V.Moskalets, Euro. Phys. Lett. **41** , 189 (1998).
- [8] T.Choi, C.M.Ryu and A.M.Jayannavar, Int. J. Mod. Phys. **B12**, 2091 (1998) and cond-mat/9808245.
- [9] S.K.Joshi, D.Sahoo and A.M.Jayannavar, Phys. Rev. B **64**, 075320 (2001).
- [10] C. Benjamin, S.K.Joshi, D.Sahoo and A. M. Jayannavar, Mod. Phys.Lett. B **15**, 19 (2001).
- [11] J.Yi et al., Phys. Rev. B **65**, 033305 (2001).
- [12] H.Wu et al., Phys. Rev. B **68**, 125330 (2003).
- [13] C. Benjamin and A.M.Jayannavar, Phys. Rev. B **64**, 2333406 (2001).
- [14] C. Benjamin and A.M.Jayannavar, Int. J. Mod. Phys. B **16**, 1787 (2002).
- [15] G. Cernicchiaro , T. Martin , K. Hasselbach¹, D. Mailly and A. Benoit , Phys. Rev. Lett. **79** , 273-276 (1997).
- [16] Hisashi Aikawa, Kensuke Kobayashi, Akira Sano, Shingo Katsumoto and Yasuhiro Iye , cond-mat/0309084
- [17] M. Büttiker , Y. Imry , and R. Landauer , Phys. Lett. **96 A**, 365 (1983).
- [18] L.P.Levy et al., Phys. Rev. Lett. **64**, 2074 (1990).
- [19] M. Büttiker , Phys. Rev.B **32**, 1846 (1985).
- [20] B. Shapiro, Phys. Rev. Lett. **50** , 747 (1983).
- [21] P.F.Bagwell, Phys. Rev. B **41**, 10354(1990).
- [22] P. Singha Deo, S. Bandopadhyay, S. Das, Int. J. Mod. Phys. B **16**, 2247 (2002).
- [23] C. Benjamin, A. M. Jayannavar, cond-mat/0309133v2 .
- [24] S. Bandopadhyay, P. Singha Deo, Phys. Rev. B **68**, 113301 (2003).
- [25] M. Büttiker, Y. Imry and R. Landauer, Phys. Lett. **96A**, 365 (1983); M. Büttiker, in *Squid '85-Superconducting Quantum Interference Devices and Their Application*, edited by H. D. Hahlbohm and H. Lüebbig (de Gruyter, Berlin, 1985); H. F. Cheung and E. K. Riedel, Phys. Rev. B **40**, 9498 (1989);
- [26] A. M. Jayannavar, P. Singha Deo and T. P. Pareek, Physica B **212** 216 (1995); A. M. Jayannavar and P. Singha Deo , Phys. Rev.B **49**, 13685 (1994).